Robust Fault-tolerant Placement of Wireless Chargers for Directional Charging

Jia Xu, *Senior Member, IEEE,* Kaijun Zhou, Sixu Wu, Haipeng Dai, *Senior Member, IEEE,* Lijie Xu, Linfeng Liu, *Member, IEEE*

Abstract—Wireless Power Transmission (WPT) has been widely used to replenish energy for wireless rechargeable sensor networks. This paper concerns the fundamental issue of robust fault-tolerant placement of wireless chargers for directional charging. Following the general directional charging model, we formulate the *Charger Placement for Robust Coverage (CPRC)* problem, which has continuous and infinite constraints, for resisting the wireless charger failure. We transform the problem to the equivalent integer program problem without performance loss by area partition and dominating strategy extraction. We show that the greedy algorithm achieves the logarithmic approximation ratio. We further formulate the *Charger Placement for Robust Utility (CPRU)* problem for resisting the sensor node failure. This problem also has continuous and infinite constraints. We transform the problem to the combinational optimization problem with finite strategy space through the techniques of charging power approximation, area discretization and dominating strategy extraction. We present the algorithm, which utilizes the combination of binary search and greedy algorithm, to solve the *CPRU* problem. We conduct both simulations and field experiments to validate our theoretical results. The simulation results show that the proposed algorithms for *CPRC* and *CPRU* can outperform comparison algorithms by at least 17.48% and 21.15%, respectively.

Index Terms—robustness, fault-tolerant, directional charging, wireless power transfer, approximation algorithm.

1 Introduction

Wireless Power Transfer (WPT) technology has been developed rapidly in recent years. Wireless Power Consortium (WPC), an organization that aims to promote worldwide compatibility of all wireless chargers and wireless power sources, has more than 400 member companies in 2021 all over the world, including Apple Inc, General Electric, General Motors, Google and so on. According to the recent report of WPC, WPT technology has been used in many applications such as laptops, tablets, drones, robots, connected cars and the intelligent cordless kitchens. There have been more than 8,000 WPT products by 2020, including wireless charging pad, car wireless charger, desktop stand and so on [1]. Furthermore, WPT technology has been used in natural disaster relief and hazardous environment exploration [2], wireless sensing platform [3, 4], public transport [5, 6], and underwater high-power transfer system [7]. In 2020, the market of WPT has grown to 17.04 billion [8].

There have been a large body of works on static wireless charger placement or scheduling [9-11], and most of them considered the placement of omnidirectional wireless chargers. In practice, most of WPT products have directional antennas [12]. The directional antenna can radiate or receive greater power in specific directions, providing improved performance over the omnidirectional antenna [13]. Based on the experiments in [14], using directional antennas can achieve performance gain by three or more times of that using omnidirectional antennas.

However, few of them considered the robustness of charger placement. Robustness is the ability of the system to survive under abnormal and dangerous conditions. Dai *et al.* [15] studied the robustly safe charging problem that considered the jitter of aroused *Electromagnetic Radiation (EMR)* of wireless chargers. Wang *et al.* [16] studied the robustly charging power problem while taking the charging power jitter into consideration. However, they did not consider the robustness for resisting system failures of both sensing network and charging network.

Both wireless chargers and sensor nodes have a large number of electronic components [17], which may break down due to various failures, such as packaging failures, contact failures, printed circuit board failures, relay failures and so on [18]. Further, the external environment may also result in system failures. For example, lightning can create an electromagnetic pulse energy and damage the wireless chargers or sensor nodes by generating over-voltage and power surges. The dust also affects the reliability of *printed circuit board assemblies (PCBAs)* [19]. Moreover, human and non-human failures can occur due to vibration, aging, corrosion, moisture, heat and cold, and bump [20].

In this paper, we study the problem of robust fault-tolerant placement of directional wireless chargers for resisting both wireless charger failure and sensor node failure. For the first case, we expect that each sensor node can receive non-zero power from multiple chargers. Thus, the failure of the minority of chargers cannot influence the whole charging system because the sensor nodes can be charged by other chargers. For the second case, we observe that sensor nodes are deployed redundantly and some sensor nodes perform the same sensing task in most sensor networks.

- *J. Xu, K. Zhou, S. Wu, L. Xu and L. Liu are with the Jiangsu Key Laboratory of Big Data Security and Intelligent Processing, Nanjing University of Posts and Telecommunications, Nanjing, Jiangsu 210023, China. (E-mail: xujia@njupt.edu.cn, 1019041113@njupt.edu.cn, 2021070711@njupt.edu.cn, ljxu@njupt.edu.cn, liulf@njupt.edu.cn).*
- *H. Dai is with the State Key Laboratory for Novel Software Technology, Nanjing University, Nanjing, Jiangsu 210023 China. (E-mail:haipengdai@nju.edu.cn).*
- *Corresponding author: Linfeng Liu*

Thus, we expect to distribute the replenished energy evenly among the sensor nodes. In other words, the objective is to maximize the minimum of charging utility of sensor nodes. By this way, the failure of the minority of sensor nodes cannot influence the whole sensing system because the other sensor nodes that perform the same sensing task are still working.

The main technical challenges are summarized as follows. First, the chargers can be placed anywhere of a 2D plane with any orientation in $[0, 2\pi)$. Thus the placement strategy space is continuous and infinite. Second, following the general charging model, the charging power is nonlinear with distance. Thus the problem of maximizing the minimum charging utility is essentially nonlinear. Moreover, maximizing the minimum of multiple set functions is not submodular, even the set functions are submodular. This brings the challenge to our optimization problem.

The main contributions of our work are summarized as follows:

- To the best of our knowledge, this is the first work to study the issue of robust fault-tolerant placement of wireless chargers.
- We formulate the *Charger Placement for Robust Coverage (CPRC)* problem for resisting the wireless charger failure and transform the problem to the equivalence integer program problem without performance loss through area partition and dominating strategy extraction. We show that the greedy algorithm can hold the logarithmic approximation ratio for our *CPRC* problem.
- We formulate the *Charger Placement for Robust Utility (CPRU)* problem for resisting the sensor node failure. This problem has continuous and infinite constraints. We transform the problem to the combinational optimization problem with finite strategy space by charging power approximation, area discretization and dominating strategy extraction.
- We transform the reformulated *CPRU* problem, and solve the problem of maximizing the minimum of multiple submodular functions with cardinality lower bound through integrating approximation algorithm for submodular covering problem and binary search.
- We conduct extensive simulations and field experiments. The results show that the proposed algorithms for *CPRC* and *CPRU* can outperform the other algorithms by at least 17.48% and 21.15%, respectively.

The rest of this paper is organized as follows. We review the state-of-art research in Section 2. We present our system model and formulate the problems in Section 3. The details of algorithm design for *CPRC* problem and *CPRU* problem are presented in Section 4 and Section 5, respectively. Extensive simulations are conducted in Section 6. Field experiments are shown in Section 7. We discuss the mobility problem of wireless chargers in Section 8 and conclude the paper in Section 9.

2 Related Work

Wireless charging technologies. There have been many wireless charging technologies, including Radio Frequency (RF) [14, 21], magnetic resonance [22] and inductive coupling [23], *etc*. In addition, Simultaneous Wireless Information and Power Transfer (SWIPT) [24, 25, 26], which can transmit signals and energy simultaneously, has also been widely studied in recent years. Boshkovska *et al.* [24] proposed a practical non-linear energy harvesting model and designed a resource allocation algorithm for the SWIPT system. According to energy harvesting model of [24], Kumar *et al.* [25] explored the performance of a SWIPT enabled cooperative Cognitive Radio Sensor Network (CRSN) over generalized *Nakagami-m* faded channels. However, the beamforming vector and the channel matrix between the transmitter and receiver are needed to calculate the power. In the charging system of this paper, there are multiple transmitters and receivers with different charging distance, thus, a large number of tests are needed, which largely affects the applicability in large-scale networks. Baek *et al.* [26] maximized the lifetime of wireless charging sensor networks based on SWIPT and the energy harvesting model. However, their model is not a directional charging model. In our paper, the orientation of charger is an important strategy of charger placement. Moreover, our scenario only involves charging and does not involve information transmission. In addition, the objective of our study is to guarantee or improve the robustness of charging system for resisting the sensor node failure or wireless charger failure, and the energy harvesting model is not needed. Therefore, we use the widely used classical RF wireless charging model from [14], which can be conveniently characterized through sampling and has been verified in our field experiments.

Omnidirectional wireless charger placement. Wu *et al.* [22] presented a multi-hop wireless charging model and formulated the problem of minimizing the comprehensive cost such that the energy demand of all sensor nodes can be fulfilled by the energy capacitated chargers. In [27], Wu *et al.* studied the placement of multi-hop wireless chargers and proposed a two-stage approach to minimize the comprehensive cost. However, both researches adopted magnetic resonance wireless charging technology rather than RF wireless charging technology. Ding *et al.* [28] studied the practical issue of deploying wireless chargers to maximize the total achieved task utility with limited deployment cost budget. However, these researches only considered the scenario of omnidirectional wireless charging, and the charging direction was not involved.

Directional wireless charger placement. Dai *et al.* [14] first presented the techniques to approximate non-linear charging power and developed dominating coverage set extraction method to solve the directional wireless charger placement problem. Ding *et al.* [29] focused on finding the strategy for placing wireless chargers from a given candidate location set to minimize the total number of placed chargers such that each sensor node's energy requirement can be fulfilled. They addressed the problem under both omnidirectional and directional charging models. Ding *et al.* [30] also investigated the cost-minimum charger placement problem under two typical scenarios in which om-

nidirectional chargers and directional chargers are used, respectively. Although these work studied the placement of directional wireless chargers, they ignored the possible failures of the sensor nodes and the wireless chargers.

Deploying mobile chargers for static rechargeable devices. Xu *et al.* [31] utilized the multiple mobile chargers to speed up charging significantly. The authors formulated a novel delay minimization problem and used an approximation algorithm to solve it. In order to maximize charging utility, Ma *et al.* [32] utilized a mobile charger to charge multiple sensor nodes simultaneously under the energy capacity constraint of the mobile charger. Xu *et al.* [33] utilized the mobile charger to charge sensor nodes so that the sum of lifetimes of sensor nodes is maximized while the travel distance of the mobile charger is minimized. However, the above studies did not take the charging cost into consideration. Priyadarshani *et al.* [34] proposed a multi-node charging vehicle scheduling scheme using partial charging model to minimize the travel energy, however, the robustness cannot be guaranteed.

Robust placement of wireless chargers. In recent years, some articles studied the robustness of the placement of wireless charger. Dai *et al.* [15] scheduled the placement of chargers so that the total charging utility of all rechargeable devices was maximized while the probability that *EMR* anywhere does not exceed the threshold was not less than a given confidence. Wang *et al.* [16] determined the orientations of the wireless chargers to maximize the overall expected charging utility while taking the charging power jittering into consideration. Both of them considered the jitter phenomenon where the *EMR* or the charging power varies in a range, rather than remaining constant. Lin *et al.* [35] studied the problem of maximizing the charging utility under specific energy constraints with the presence of obstacles. However, the robustness problems studied above are extremely different with that in this paper. In this paper, we study the fault-tolerant wireless charger placement to resist both wireless charger failure and sensor node failure, improving the robustness of sensing system and charging system.

3 System Model and Problem Formulation

3.1 System Model

We consider a rechargeable sensor network consisting of a set of rechargeable sensor nodes $S = \{s_1, s_2, ..., s_n\}$ deployed with any orientation in a 2D plane Ω. A set of wireless chargers O can be placed anywhere with any orientation in the plane.

Each wireless directional charger has a charging radius D and a charging angle A_s. Each sensor node has a receiving radius D and a receiving angle A_o. Any charger $o_j \in O$ with orientation vector $\overrightarrow{r_{\theta_j}}$ only charges sensor nodes in a charging area in the shape of a sector with charging angle A_s and charging radius D. A rechargeable sensor node s_i with orientation vector $\overrightarrow{r_{\phi_i}}$ only receives power in a receiving area in the shape of a sector with receiving angle A_o and the same radius D. As illustrated in Fig. 1, the sensor node s_2 can be charged by wireless charger o_1. Nevertheless, the sensor node s_1 cannot be charged by wireless charger o_1 since its receiving area does not cover o_1.

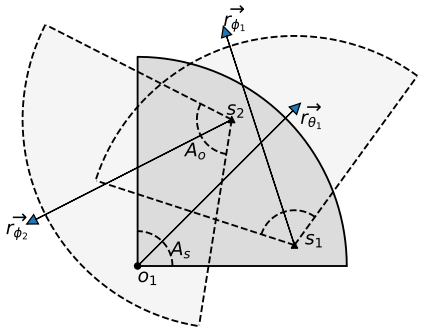

Fig. 1. Directional charging model.

By incorporating the widely accepted empirical directional charging model [14], the charging power from the wireless charger $o_j \in O$ to the sensor node $s_i \in S$ can be given by

$$P(s_i, o_j, \phi_i, \theta_j) = \begin{cases} \frac{\alpha}{(d(s_i,o_j)+\beta)^2}, & d(s_i, o_j) \le D, \\ & \overrightarrow{o_j s_i} \cdot \overrightarrow{r_{\theta_j}} - d(s_i, o_j)\cos(A_s/2) \ge 0, \\ & \overrightarrow{s_i o_j} \cdot \overrightarrow{r_{\phi_i}} - d(s_i, o_j)\cos(A_o/2) \ge 0 \\ 0, & otherwise \end{cases} \tag{1}$$

where $d(s_i, o_j)$ is the distance between sensor node s_i and wireless charger o_j. ϕ_i and θ_j are the orientations of sensor node s_i and placed wireless charger o_j, respectively. $\overrightarrow{r_{\theta_j}}$ and $\overrightarrow{r_{\phi_i}}$ are the unit vectors standing for the orientations of the charger o_j and the sensor s_i. α and β are two constants determined by the environment and hardware parameters of chargers [14, 17].

The fading effect caused by multi-path propagation, shadowing from obstacles, *etc*, will lead to power jitter [15]. Although SWIPT [24, 25, 26] has also been widely studied in recent years, the beamforming vector and the channel matrix between the transmitter and receiver are needed to calculate the power, which largely affects the applicability in large-scale networks. Moreover, SWIPT model is not a directional charging model. In our paper, the orientation of charger is an important strategy of charger placement. In addition, our scenario only involves charging and does not involve information transmission. Therefore, we use the widely used classical RF wireless charging model from [14], which can be conveniently characterized through sampling and has been verified in our field experiments.

3.2 Problem Formulation

For convenience, we still use o_j to denote the position of charger o_j. Let tuple (o_j, θ_j) denote the position o_j and orientation θ_j of the charger o_j, i.e., the placement strategy of the charger. Let $\mathcal{H}$ denote the strategy space, i.e., the set of all possible placement strategies of chargers. Considering the fact that the chargers can be placed anywhere with continuous orientations in [0,2π), the possible strategies are infinite. Let $\mathcal{H}_s \subseteq \mathcal{H}$ denote the strategy set of placed chargers. Further, we define 0-1 variable $x(o_j, \theta_j)$ to indicate whether the placement strategy (o_j, θ_j) is included in $\mathcal{H}_s$,

i.e., $x(o_j, \theta_j) = 1$ if $(o_j, \theta_j) \in \mathcal{H}_s$, $x(o_j, \theta_j) = 0$ otherwise. We define $S(o_j, \theta_j)$ as the set of sensor nodes that can receive non-zero power by the placement strategy (o_j, θ_j).

For resisting the wireless charger failure, we aim to minimize the number of wireless chargers such that each sensor node s_i can receive non-zero power from at least λ_i wireless chargers, where λ_i is the coverage demand and is determined by the importance of s_i, e.g., the value, rareness or urgency of data sensed by s_i. We define the *CPRC* problem as follows:

$$\textbf{(P1)} \quad min \sum_{(o_j,\theta_j)\in\mathcal{H}} x(o_j, \theta_j) \tag{2}$$

$$s.t. \sum_{(o_j,\theta_j),s_i\in S(o_j,\theta_j)} x(o_j, \theta_j) \geq \lambda_i, \quad \forall s_i \in S \tag{3}$$

$$o_j \in \Omega, \quad 0 \leq \theta_j < 2\pi \tag{4}$$

The constraint (3) ensures that each sensor node s_i can receive non-zero power from at least λ_i wireless chargers. The constraint (4) ensures that the chargers can be placed anywhere with any orientation.

For resisting the sensor node failure, we aim to maximize the minimum charging utility of all sensor nodes with limited number of chargers. The rechargeable sensor nodes have the upper bounds of charging power [14] because they must prevent from the overload that could damage the sensor nodes [36]. Given the strategy set of placed chargers $\mathcal{H}_s$, the charging utility for sensor node s_i is given by:

$$U_i(\mathcal{H}_s) = min\{\sum_{(o_j,\theta_j)\in\mathcal{H}_s} P(s_i, o_j, \phi_i, \theta_j), P_i^{max}\} \tag{5}$$

where P_i^{max} is the maximum charging power of sensor node s_i.

The objective is to maximize the minimum charging utility of all sensor nodes. The charging utility under strategy set $\mathcal{H}_s$ is given by:

$$U(\mathcal{H}_s) = min_{s_i\in S} U_i(\mathcal{H}_s) \tag{6}$$

We formulate the *CPRU* problem as follows:

$$\textbf{(P2)} \quad max \quad U(\mathcal{H}_s) \tag{7}$$

$$s.t. \quad |\mathcal{H}_s| \leq m, \mathcal{H}_s \subseteq \{(o_j, \theta_j) | o_j \in \Omega, 0 \leq \theta_j < 2\pi\} \tag{8}$$

The constraint (8) ensures that the number of placed chargers is not larger than m.

We list the frequently used notations in TABLE 1.

TABLE 1
Frequently Used Notations

Symbol	Description
S, O	Set of rechargeable sensor nodes, set of wireless chargers
$d(s_i, o_j)$	Distance between sensor node s_i and wireless charger o_j
m, n	Maximum number of wireless chargers, number of sensor nodes
A_o, A_s, D	Receiving angle of sensor nodes, charging angle of wireless chargers, charging radius
$P(\cdot)$	Charging power function
θ_j, ϕ_i	Orientation of wireless charger o_j, orientation of sensor nodes s_i
α, β	Constants in the charging model
$\mathcal{H}, \mathcal{H}_s$	Strategy space, strategy set of placed chargers
(o_j, θ_j)	Placement strategy of the charger placed in position o_j with orientation θ_j
$S(o_j, \theta_j)$	Set of sensor nodes that can receive non-zero power from the placement strategy (o_j, θ_j)
S_p	Coverage set of subarea C_p
λ_i	Coverage demand of sensor node s_i
P_i^{max}	Maximum charging power of sensor node s_i
$U_i(\cdot), U(\cdot)$	Charging utility of sensor node s_i, charging utility of all sensor nodes

4 Solution for CPRC Problem

In this section, we present the algorithm to solve the *CPRC* problem.

4.1 Hardness and Design Rationale

First of all, we attempt to find an optimal algorithm for the *CPRC* problem. Unfortunately, as the following theorem shows, the *CPRC* problem is NP-hard.

Theorem 1. *The CPRC problem is NP hard.*

Proof: We consider the special case of *CPRC* problem, where the possible charger placement strategies are finite. Then the problem changes to finding the least positions for placing chargers such that each sensor node s_i can be covered by λ_i chargers. This problem is the set multi-cover problem, where each set can be picked more than once. Obviously, this problem is a generalization of the well-known NP-hard set cover problem [37][38]. Since the set multi-cover problem is NP-hard, the *CPRC* problem is NP-hard. ■

As shown in Theorem 1, the *CPRC* problem is essentially the set multi-cover problem if the strategy space is finite, and can be solved by the approximation algorithm following greedy approach [37][38]. Thus, we first partition the area into subareas to get finite subareas to place chargers. Then, we find the dominating strategies for each subarea to get finite strategies of charger placement. By this way, the continuous search space of strategies of chargers is reduced to a limited number of strategies without performance loss. Finally, the greedy algorithm with approximation ratio of $(\ln n + 1)$ for set cover problem is employed to address the *CPRC* problem. We show that the approximation ratio of greedy algorithm still holds for our *CPRC* problem.

4.2 Area Partition and Dominating Strategy Extraction

Since a rechargeable sensor node only receives power in a receiving area in the shape of a sector, we partition the 2D plane to subareas by the receiving areas of sensor nodes. As shown in Fig. 2, there are three sensor nodes with three receiving areas. The 2D plane is partitioned to 7 subareas.

Based on Lemma 5 of [14], we have the following Lemma.

Lemma 1. *The number of partitioned subareas for n uniform sections is not larger than $5n^2 - 5n + 2$.*

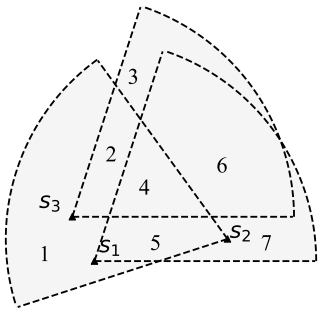

Fig. 2. Area partition based on the receiving areas of sensor nodes.

For the *CPRC* problem, we only need to consider the coverage relationship between chargers and sensor nodes in each subarea, which depends on both positions and orientations of chargers.

To begin with, we give the definition of dominating strategy.

Definition 1.*(Dominating Strategy): Given a set of sensor nodes $S(o_j, \theta_j)$, if there doesn't exist a strategy $(o_{j'}, \theta_{j'})$ such that $S(o_j, \theta_j) \subset S(o_{j'}, \theta_{j'})$, then (o_j, θ_j) is a dominating strategy.*

In what follows, we aim to extract dominating strategies for each subarea. We first consider the special case where the subarea becomes a position. We then study the general case.

(1) Dominating Strategy Extraction for Position Case

For each position, we rotate the orientation of charger from 0 to 2π widdershins to cover sensor nodes one by one. We first initialize the orientation of the charger as 0°. During the rotating process, if there is some covered sensor node going to be uncovered, the current strategy consisting of current orientation and position is marked as a dominating strategy. And then keep rotating, if there is some covered sensor node going to be uncovered after a new sensor node is covered, the current strategy is marked as a dominating strategy. During the rotating process, if the rotated angle is larger than 2π, terminate the rotating. Obviously, for any of unmarked strategies, there must be at least one dominating strategy, which can cover the same set of sensor nodes.

As illustrated in Fig. 3(a), the rotation starts at 0°, and the charger covers s_1 and s_2. By rotating the charger widdershins, s_1 goes to be uncovered on the orientation illustrated in Fig. 3(b). s_3 cannot be added in the current covered set as otherwise $\{s_1, s_2\}$ will be missed. Thus, the strategy illustrated in Fig. 3(b) is a dominating strategy. Then, the charger keeps rotating and covers new sensor nodes s_3 and s_4 sequentially. When s_3 goes to be uncovered, the strategy illustrated in Fig. 3(c) is a dominating strategy. Similarly, the strategy illustrated in Fig. 3(d) is also a dominating strategy. Continue the rotating process until the charger rotates for 360°. Therefore, there are 3 dominating strategies in this example.

(2) Dominating Strategy Extraction for Subarea Case

First, we give the definition of coverage set of subarea.

Definition 2. *(Coverage Set of Subarea): The coverage set S_p of any subarea C_p are the sensor nodes that can receive non-zero power by a charger in C_p.*

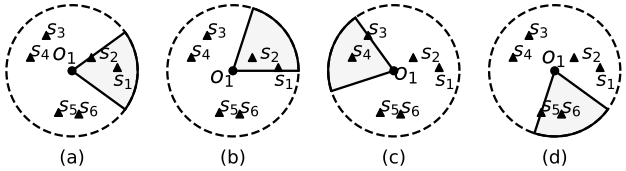

Fig. 3. Illustration of dominating strategy extraction for position case.

Obviously, for any dominating strategy (o_j, θ_j) in subarea C_p, $S(o_j, \theta_j)$ is a subset of the coverage set of C_p.

The dominating strategy extraction for a give subarea C_p is illustrated in Algorithm 1. Fig. 4 shows an example of how the algorithm works. Given the subarea and corresponding coverage set with six sensors as shown in Fig. 4(a), we first draw lines passing through each pair of sensor nodes, such as s_1 and s_2 in Fig. 4(b), and cross the boundaries of the subarea at positions o_1 and o_2, then we obtain two candidate dominating strategies (o_1, θ_1) and (o_2, θ_1) with $S(o_1, \theta_1) = \{s_1, s_2, s_3\}$ and $S(o_2, \theta_1) = \{s_1, s_2, s_3, s_6\}$, respectively. Next, we construct a charging angel A_s with two boundaries passing through each pair of sensor nodes like s_3 and s_4 as shown in Fig. 4(c), and adjust A_s such that the vertex of A_s lie rightly on the boundaries of subarea at positions o_3 and o_4. Then we obtain two candidate dominating strategies (o_3, θ_2) and (o_4, θ_3) with $S(o_3, \theta_2) = \{s_3, s_4, s_5\}$ and $S(o_4, \theta_3) = \{s_3, s_4, s_6\}$, respectively. Finally, as illustrated in Fig. 4(d), we randomly choose a position o_5 on the boundaries and perform the algorithm for dominating strategy extraction for position case to further find three candidate dominating strategies (o_5, θ_4), (o_5, θ_5) and (o_5, θ_6) with $S(o_5, \theta_4) = \{s_1, s_2, s_6\}$, $S(o_5, \theta_5) = \{s_2, s_3, s_6\}$ and $S(o_5, \theta_6) = \{s_4, s_5\}$, respectively. At the final step, $\{s_1, s_2, s_3\}$, $\{s_1, s_2, s_6\}$, $\{s_2, s_3, s_6\}$, $\{s_4, s_5\}$ can be removed as they are subsets of $\{s_1, s_2, s_3, s_6\}$ or $\{s_3, s_4, s_5\}$.

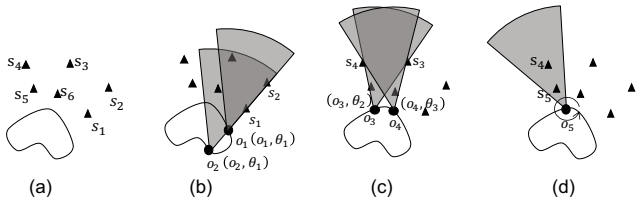

Fig. 4. Dominating strategy extraction for a give subarea.

Denote the dominating strategy set obtained from Algorithm 1 by $\mathcal{H}_f$, then we have the following theorem.

Theorem 2. *Given any strategy (o_j, θ_j), there must exist $(o_{j_3}, \theta_{j_3}) \in \mathcal{H}_f$ such that $S(o_{j_3}, \theta_{j_3}) \supseteq S(o_j, \theta_j)$.*

Proof: Given a strategy (o_j, θ_j), we move the charger along the reverse direction of its orientation until reaching some point o_{j_1} on the boundary of the subarea. Suppose the obtained strategy is (o_{j_1}, θ_{j_1}), where $\theta_{j_1} = \theta_j$. Obviously, we have $S(o_{j_1}, \theta_{j_1}) \supseteq S(o_j, \theta_j)$.

Then, we fix the position o_{j_1}, and rotate the charger anticlockwise such that there is at least one sensor node, say s_1, touching the right boundary of the charging area.

Algorithm 1 Dominating Strategy Extraction for Subarea Case

Input: subarea C_p, coverage set S_p
Output: dominating strategy set of subarea C_p

1: **for each** pairs of sensor node, say s_1 and s_2, in S_p **do**
2: Draw a straight line passing through s_1 and s_2 and extend the line to intersect with the boundaries of subarea C_p. Let s_1 and s_2 lie rightly on its charging area's clockwise boundary. Then insert all strategies under current setting into the candidate dominating strategy set.
3: Form a charging angel A_s with two boundaries passing through s_1 and s_2, respectively. Adjust A_s such that the vertex of A_s lie rightly on the boundaries of subarea C_p. Then insert all strategies under current setting into the candidate dominating strategy set.
4: **end for**
5: Randomly select a position o_j at the boundary of the subarea, perform the algorithm for dominating strategy extraction for position case and add the results to the candidate dominating strategy set.
6: Remove the strategies that are subsets of some dominating strategies in the candidate dominating strategy set.

Suppose the obtained strategy is (o_{j_2}, θ_{j_2}), where $o_{j_2} = o_{j_1}$. Obviously, we have $S(o_{j_2}, \theta_{j_2}) \supseteq S(o_{j_1}, \theta_{j_1})$.

Afterwards, we move the charger along the subarea's boundaries and change its orientation accordingly, and guarantee that: (1) the newly obtained strategy (o_{j_3}, θ_{j_3}) satisfies $S(o_{j_3}, \theta_{j_3}) \supseteq S(o_{j_2}, \theta_{j_2})$; and (2) the clockwise boundary of the charging area must cross s_1. Apparently, (o_{j_3}, θ_{j_3}) falls into one of the three possible situations as shown in Fig. 5.

Case 1: At some position o_{j_3} on the boundary of the subarea, there is some sensor node, e.g., s_2 in Fig. 5(a), that touches the clockwise boundary of the charging area of (o_{j_3}, θ_{j_3}).

Case 2: At some position o_{j_3} on the boundary of the subarea, there is some sensor node, e.g., s_3 in Fig. 5(b), that touches the anticlockwise boundary of the charging area of (o_{j_3}, θ_{j_3}).

Case 3: Neither Case 1 nor Case 2 occurs for any position o_{j_3} on the boundary of the subarea. (as shown in Fig. 5(c)).

The Line 2 of Algorithm 1 corresponds to Case 1. The Line 3 of Algorithm 1 corresponds to Case 2. In Line 5 of Algorithm 1, randomly selecting a position on the subarea's boundaries and extracting the dominating strategies for position case can find all the dominating strategies resulted from Case 3. Thus, we have $(o_{j_3}, \theta_{j_3}) \in \mathcal{H}_f$. Since $(o_{j_3}, \theta_{j_3}) \supseteq S(o_{j_2}, \theta_{j_2}) \supseteq S(o_{j_1}, \theta_{j_1}) \supseteq S(o_j, \theta_j)$, we get the theorem. ■

Lemma 2. *The number of dominating strategies for any subarea is $O(n^2)$.*

Proof: By Algorithm 1, for either Case 1 (Line 2) or Case 2 (Line 3) in each subarea, the number of candidate dominating strategies is $O(n^2)$ since the number of sensor node pairs is $C_n^2 = \frac{(n(n-1))}{2}$ and each case generates only $O(1)$ number of candidate dominating strategies. For Case 3 (Line 5), there are $O(n)$ candidate dominating strategies since there are at most n sensor nodes in the coverage set of any subarea. Thus, there are $O(n^2)$ dominating strategies for any subarea. ■

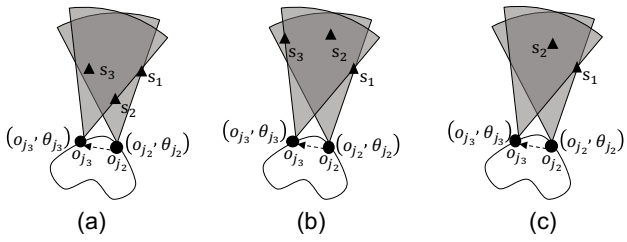

Fig. 5. Three situations in the proof of Theorem 2.

After area partition and dominating strategy extraction, the *CPRC* problem can be reformulated as:

$$\textbf{(P3)} \quad min \sum_{(o_j,\theta_j)\in\mathcal{H}_f} x(o_j,\theta_j) \tag{9}$$

$$s.t. \sum_{(o_j,\theta_j),s_i\in S(o_j,\theta_j)} x(o_j,\theta_j) \geq \lambda_i, \quad \forall s_i \in S \tag{10}$$

4.3 Approximation Algorithm for CPRC

We present the approximation algorithm for *CPRC* problem. Since the strategy space is finite after area partition and finding dominating orientations, we employ the greedy algorithm for set cover problem to solve the *CPRC* problem.

Algorithm 2 Approximation Algorithm for *CPRC* Problem

Input: strategy space $\mathcal{H}_f$, set of sensor nodes S
Output: strategy set of placed chargers $\mathcal{H}_s$

1: $\mathcal{H}_s \leftarrow \varnothing$;
2: **for each** $s_i \in S$ **do**
3: $\lambda_i' \leftarrow \lambda_i$
4: **end for**
5: **while** $\sum_{s_i\in S} \lambda_i' \neq 0$ **do**
6: $(o_j, \theta_j) \leftarrow \arg max_{(o_h,\theta_h)\in\mathcal{H}_f} \sum_{s_i\in S(o_h,\theta_h)} min\{1, \lambda_i'\}$;
7: $\mathcal{H}_s \leftarrow \mathcal{H}_s \cup \{(o_j, \theta_j)\}$;
8: **for each** $s_i \in S(o_j, \theta_j)$ **do**
9: $\lambda_i' \leftarrow \lambda_i' - min\{1, \lambda_i'\}$;
10: **end for**
11: **end while**

As illustrated in Algorithm 2, the placement strategies are sorted according to the effective coverage. Given the remaining multiplicity of each sensor node λ_i', $s_i \in S(o_h, \theta_h)$, the effective coverage of sensor node s_i is $min\{1, \lambda_i'\}$. The effective coverage of placement strategy (o_h, θ_h) is defined as $\sum_{s_i\in S(o_h,\theta_h)} min\{1, \lambda_i'\}$. In each iteration of while-loop (Lines 5-11), we select the placement strategy with the maximum effective coverage in the strategy space $\mathcal{H}_f$ (Line 6) until the coverage can meet the requirement of multiplicity of each sensor node in S.

Theorem 3. *The time complexity of approximation algorithm for CPRC problem is $O(n^5 \sum_{s_i\in S} \lambda_i)$.*

Proof: Let $|\mathcal{H}_f|$ be the size of strategy space, then finding placement strategy with the maximum effective coverage takes $O(|\mathcal{H}_f|n)$, where computing the value of

$\sum_{s_i \in S(o_h,\theta_h)} min\{1, \lambda'_i\}$ takes $O(n)$ time. Hence, the while-loop (Lines 5-11) takes $O(|\mathcal{H}_f| n \sum_{s_i \in S} \lambda'_i)$. This is because the total multiplicities of all sensor nodes is $\sum_{s_i \in S} \lambda'_i$, and each placed charger can achieve at least 1 multiplicity. Based on Lemma 1 and Lemma 2, the size of $\mathcal{H}_f$ is $O(n^4)$. Since the while-loop (Lines 5-11) dominates the whole algorithm, the time complexity of algorithm for *CPRC* problem is $O(n^5 \sum_{s_i \in S} \lambda_i)$. ■

Since the *CPRC* problem with finite strategy space is equivalent to the set multi-cover problem, we have the following theorem.

Theorem 4. *The algorithm for CPRC problem achieves the approximation ratio of $\mathcal{H}_n$, where H_n is harmonic function.*

5 Solution for CPRU Problem

In this section, we present the algorithm to solve the *CPRU* problem defined in (P2).

5.1 Hardness and Property of CPRU Problem

Theorem 5. *The CPRU problem is NP hard.*

Proof: Since the objective function of *CPRU* problem is nonlinear and the strategy space is infinite, *CPRU* falls in the realm of nonlinear programming, which is NP-hard [39]. ■

To analyze the property of *CPRU* problem, we give the following definition.

Definition 3. *(Nonnegative, monotone, and submodular function): Given a finite ground set V, a real-valued set function defined as $f : 2^V \to \mathbb{R}$, f is called nonnegative, monotone, and submodular if and only if it satisfies following conditions, respectively:*

$f(\emptyset) = 0$ and $f(A) \geq 0$ for all $A \subseteq V$;

$f(A) \leq f(B)$ for all $A \subseteq B \subseteq V$;

$f(A) + f(B) \geq f(A \cup B) + f(A \cap B)$ for any $A, B \subseteq V$ or equivalently: $f(A \cup \{e\}) - f(A) \geq f(B \cup \{e\}) - f(B)$, $A \subseteq B \subseteq V$, $e \in V \setminus B$.

Theorem 6. *For any sensor node s_i, the function $U_i(\cdot)$ is a nonnegative, monotone, and submodular function.*

Proof: For any $A \subseteq B \subseteq V$ and $(o_j, \theta_j) \in V \setminus B$, we have following two cases:

Case 1: $U_i(A) = P_i^{max}$.

Because $A \subseteq B$, we have $U_i(B) = U_i^{max}$. Thus, $U_i(A \cup \{(o_j, \theta_j)\}) - U_i(A) = U_i(B \cup \{(o_j, \theta_j)\}) - U_i(B) = 0$.

Case 2: $U_i(A) < U_i^{max}$.

We further have following two subcases:

Case 2.1: $U_i(B) = U_i^{max}$.

Because the monotonicity of function $U_i(\cdot)$, we have: $U_i(A \cup \{(o_j, \theta_j)\}) - U_i(A) \geq U_i(B \cup \{(o_j, \theta_j)\}) - U_i(B) = 0$.

Case 2.2: $U_i(B) < U_i^{max}$.

We have: $U_i(A \cup \{(o_j, \theta_j)\}) - U_i(A) = min\{P(s_i, o_j, \phi_i, \theta_j), P_i^{max} - U_i(A)\}$, $U_i(B \cup \{(o_j, \theta_j)\}) - U_i(B) = min\{P(s_i, o_j, \phi_i, \theta_j), P_i^{max} - U_i(B)\}$. We discuss the following three subcases:

Case 2.2.1: $P(s_i, o_j, \phi_i, \theta_j) \leq P_i^{max} - U_i(B)$.

Because the monotonicity of function $U_i(\cdot)$, we have $P(s_i, o_j, \phi_i, \theta_j) \leq P_i^{max} - U_i(A)$. Thus, we have $U_i(A \cup \{(o_j, \theta_j)\}) - U_i(A) = U_i(B \cup \{(o_j, \theta_j)\}) - U_i(B) = P(s_i, o_j, \phi_i, \theta_j)$.

Case 2.2.2: $P_i^{max} - U_i(B) < P(s_i, o_j, \phi_i, \theta_j) < P_i^{max} - U_i(A)$.

We have $U_i(A \cup \{(o_j, \theta_j)\}) - U_i(A) = P(s_i, o_j, \phi_i, \theta_j) > U_i(B \cup \{(o_j, \theta_j)\}) - U_i(B)$.

Case 2.2.3: $P_i^{max} - U_i(A) < P(s_i, o_j, \phi_i, \theta_j)$.

We have $U_i(A \cup \{(o_j, \theta_j)\}) - U_i(A) = P_i^{max} - U_i(A) \geq P_i^{max} - U_i(B) = U_i(B \cup \{(o_j, \theta_j)\}) - U_i(B)$. where the inequation relies on the monotonicity of function $U_i(\cdot)$.

Therefore, for each sensor node $s_i \in S$, $U_i(\cdot)$ is a nonnegative, monotone and submodular function. ■

5.2 Approximation of Charging Power

Let $P(d)$ denote the power that a sensor node receives from a charger with distance d. We use multiple piecewise constant segments $\widetilde{P}(d)$ to approximate the charging power. Let $l(0), l(1), ..., l(K)$ be the end points of K constant segments in an increasing sequence, where $l(0) = 0$ and $l(K) = D$. Then the piecewise constant function can be defined as

$$\widetilde{P}(d) = \begin{cases} P(l(1)), & d = l(0) \\ P(l(k)), & l(k-1) < d \leq l(k), k = 1, 2..., K \\ 0, & d > l(K) \end{cases} \tag{11}$$

For example, we set $K = 2$ in Fig. 6. Thus, the charging area is partitioned into 2 subareas, and any points in the same subarea have the same power.

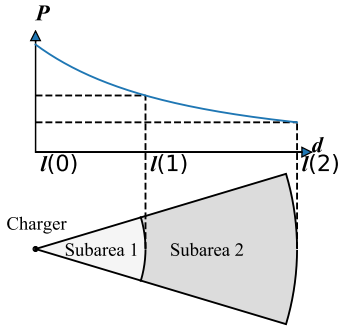

Fig. 6. Approximation of charging power, where $K = 2$. The black dotted curves stand for the approximated value of charging power.

Let ϵ denote the constant threshold to ensure that the approximation error is not larger than ϵ. We have the following theorem.

Theorem 7. *Let $l(0) = 0$, $l(K) = D$, and $l(k) = \beta((1+\epsilon)^{k/2} - 1)$, $k = 1, ..., K-1$, (therefore $K = \left\lceil \frac{ln(P(0)/P(D))}{ln(1+\epsilon)} \right\rceil$). For any $d \leq D$, we have*

$$\frac{P(d)}{\widetilde{P}(d)} \leq 1 + \epsilon \tag{12}$$

Proof: We consider the following two cases.

Case 1: $d = l(0) = 0$.

$\frac{P(d)}{\widetilde{P}(d)} = \frac{P(0)}{P(l(1))} = \frac{\alpha/\beta^2}{\alpha/(\beta((1+\epsilon)^{1/2}-1)+\beta)^2} = 1 + \epsilon$.

Case 2: $l(k-1) < d \leq l(k)$, $k = 1, 2, \ldots, K$.

$\frac{P(d)}{\widetilde{P}(d)} = \frac{P(d)}{P(l(k))} \leq \frac{P(l(k-1))}{P(l(k))} = \frac{\alpha/(\beta((1+\epsilon)^{(k-1)/2}-1)+\beta)^2}{\alpha/(\beta((1+\epsilon)^{k/2}-1)+\beta)^2} = \frac{(1+\epsilon)^k}{(1+\epsilon)^{k-1}} = 1 + \epsilon$. ■

5.3 Area Discretization

In this subsection, we bound the size of strategy space of charger placement by area discretization. We draw concentric circles with radii $l(1), l(2), ..., l(K)$ centered at each sensor node, respectively. Due to geometric symmetry, if a charger is located between two successive circles with radii $l(k)$ and $l(k+1)$ with respect to a sensor node, the sensor node must also lie between two circles with radii $l(k)$ and $l(k+1)$ centered at the charger, leading to a constant approximated charging power if the charger covers the sensor node.

By this way, the receiving area of each sensor node is divided to K subareas, and the chargers placed in the same subarea have the same approximated charging power to the sensor node. We combine the charging power discretization with the area partition presented in Section 4.2. Then the maximum number of candidate positions can be bounded. As illustrated in Fig. 7, there are 2 sensor nodes, and each receiving area of sensor node is partitioned into 3 subareas. Therefore, there are total 11 subareas in this example.

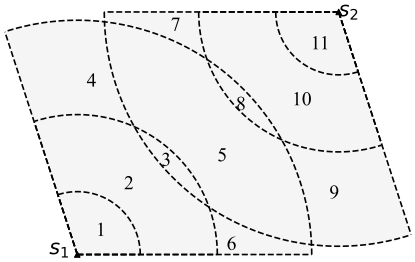

Fig. 7. Area discretization for 2 sensor nodes with $K = 3$.

Lemma 3. *The number of partitioned subareas is no more than* $5K^2n^2 - 5Kn + 2$, *where* $K = \left\lceil \frac{2ln((D+\beta)/\beta)}{ln(1+\epsilon)} \right\rceil$.

Proof: Since the receiving area of each sensor node is divided to K subareas, there are totally Kn sections which may intersect with each other in the whole 2D plane. Following Lemma 1 and Theorem 7, we can conclude that the number of partitioned subareas is not larger than $5K^2n^2 - 5Kn + 2$, where $K = \left\lceil \frac{ln(P(0)/P(D))}{ln(1+\epsilon)} \right\rceil = \left\lceil \frac{2ln((D+\beta)/\beta)}{ln(1+\epsilon)} \right\rceil$. ■

Let $\widetilde{U}_i(\mathcal{H}_s)$ and $\widetilde{U}(\mathcal{H}_s)$ denote the approximated charging utility of sensor node s_i and approximated charging utility of all sensor nodes for the strategy set $\mathcal{H}_s$, respectively. We have

$$\widetilde{U}(\mathcal{H}_s) = min_{s_i \in S} \widetilde{U}_i(\mathcal{H}_s) \tag{13}$$

$$\widetilde{U}_i(\mathcal{H}_s) = min\{ \sum_{(o_j,\theta_j) \in \mathcal{H}_s} \widetilde{P}(s_i, o_j, \phi_i, \theta_j), P_i^{max} \} \tag{14}$$

where $\widetilde{P}(s_i, o_j, \phi_i, \theta_j)$ is the approximation of $P(s_i, o_j, \phi_i, \theta_j)$.

Then, we perform dominating strategy extraction for the discretized subareas. We still denote the strategy space by $\mathcal{H}_f$, and the *CPRU* problem (P2) can be reformulated as:

$$\textbf{(P4)} \quad max \widetilde{U}(\mathcal{H}_s) \tag{15}$$

$$s.t. \quad |\mathcal{H}_s| \leq m, \quad \mathcal{H}_s \subseteq \mathcal{H}_f \tag{16}$$

5.4 Algorithm Design

Obviously, P4 is a combinational optimization problem. Specifically, $\widetilde{U}_i(\mathcal{H}_s)$ is a nonnegative, monotone, and submodular function according to Theorem 6. Therefore, P4 is to maximize the minimum of multiple submodular functions with cardinality lower bound.

We first transform P4 to P5:

$$\textbf{(P5)} \quad max \quad k \tag{17}$$

$$s.t. \quad \widetilde{U}_i(\mathcal{H}_s) \geq k, \forall s_i \in S, |\mathcal{H}_s| \leq m, \mathcal{H}_s \subseteq \mathcal{H}_f \tag{18}$$

where $k \geq 0$ is the lower bound of $min_{s_i \in S} \widetilde{U}_i(\mathcal{H}_s)$. Obviously, P4 and P5 are equivalent.

It is still difficult to solve P5 directly. We formulate P6 to find the feasible solutions of P5. For any given value of k, we find the smallest set $\mathcal{H}_k = \arg\min_{\mathcal{H}_s \subseteq \mathcal{H}_f} |\mathcal{H}_s|$ by P6. If the size of $\mathcal{H}_k$ is not larger than m, then $|\mathcal{H}_k|$ satisfies the constraints of P5. In other words, this k is a feasible solution of P5. Thus, if we search all possible solutions, $k^* = max_{|\mathcal{H}_k| \leq m} k$ is the optimal solution of P5.

$$\textbf{(P6)} \quad min_{\mathcal{H}_s \subseteq \mathcal{H}_f} |\mathcal{H}_s| \tag{19}$$

$$s.t. \quad \widetilde{U}_i(\mathcal{H}_s) \geq k, \quad \forall s_i \in S \tag{20}$$

For any given value of k, if there exists the optimal algorithm or approximation algorithm of P6, we can use binary search to find the maximum value of k under the constraints for given search accuracy. In each round of binary search, for a given k, we solve P6 to find the best $\mathcal{H}_k$, and check whether this k can satisfy the constraints in P5, so as to determine the direction of the next binary search round. Thus, we turn our attention to P4.

To solve P4, We use the constraint $\overline{U}_k(\mathcal{H}_s) = \overline{U}_k(\mathcal{H}_f)$ to replace the constraint of P6, where $\overline{U}_k(\mathcal{H}_s) = \frac{1}{n} \sum_{s_i \in S} \widehat{U}_{i,k}(\mathcal{H}_s)$, $\widehat{U}_{i,k}(\mathcal{H}_s) = min\{\widetilde{U}_i(\mathcal{H}_s), k\}$, $k > 0$. Each of $\widehat{U}_{i,k}(\cdot)$ is monotonic submodular because it is a truncated function of its corresponding monotonic submodular function $\widetilde{U}_i(\mathcal{H}_s)$. $\overline{U}_k(\mathcal{H}_s)$ is also monotonic submodular since the accumulation combination of monotonic submodular functions is also a monotonic submodular function [40].

Obviously, $\overline{U}_k(\mathcal{H}_s) = k$ if and only if $min_{s_i \in S} \widetilde{U}_i(\mathcal{H}_s) \geq k$, which indicates that P6 can be redefined to find the smallest strategy set $\mathcal{H}_s$ satisfying $\overline{U}_k(\mathcal{H}_s) = k$. From the monotonicity of $\overline{U}_k(\mathcal{H}_s)$ and the value range of k, we have $k = \overline{U}_k(\mathcal{H}_f)$. Then, we can reformulate P6 as:

$$\textbf{(P7)} \quad min_{\mathcal{H}_s \subseteq \mathcal{H}_f} |\mathcal{H}_s| \tag{21}$$

$$s.t. \quad \overline{U}_k(\mathcal{H}_s) = \overline{U}_k(\mathcal{H}_f) \tag{22}$$

P7 is an instance of *submodular covering problem* [40], which is NP-hard. Fortunately, as shown in Theorem 8, the greedy algorithm can achieve the guaranteed approximation for *submodular covering problem* [41].

Theorem 8. *Given a monotonic submodular function* F *on a ground set* Ω, *the greedy algorithm, applied to the optimization problem:*

$$min_{S \subseteq \Omega} |S| \quad s.t. \, F(S) = F(\Omega)$$

can approximate the optimal solution within a factor of $\delta = 1 + log(max_{e \in \Omega} F(\{e\}))$.

However, Theorem 8 also shows that the approximation ratio of greedy algorithm for P7 is δ. This means that, in our setting, the solution of P7 is relaxed by $\delta = 1 + log(max_{(o_j,\theta_j)\in\mathcal{H}_f}\overline{U}_k(\{(o_j,\theta_j)\}))$ for any given k. Thus we have to relax the constraint of cardinality constraint of P5 as $|\mathcal{H}_s| \leq \delta m$ to avoid losing any solution from P7. The relaxed version of P5 is formulated as P8.

$$\textbf{(P8)} \quad max \quad k \tag{23}$$

$$s.t. \quad \widetilde{U}_i(\mathcal{H}_s) \geq k, \forall s_i \in S, |\mathcal{H}_s| \leq \delta m, \mathcal{H}_s \subseteq \mathcal{H}_f \tag{24}$$

In summary, we first transform P4 to its equivalent problem P5. Next, we construct P6 for generating $\mathcal{H}_s$ for P5 by binary searching k in a valid domain. However, since P6 is still hard to solve, we use P7 to reformulate P6. P7 can be solved by a δ-approximation greedy algorithm. Thus, we relax P5 to P8, and obtain the solution for P8 through the greedy algorithm solving P7.

If we had an optimal algorithm for submodular covering problem (P7), then we would set $\delta = 1$, and the algorithm solving P7 would return the optimal solution to the *CPRU* problem. However, the greedy algorithm for P7 may make the solution unfeasible to P5 when $\delta > 1$. Thus, we set $\delta = 1$ in our designed algorithm, which works very effectively in our experiments.

The algorithm for *CPRU* problem is illustrated in Algorithm 3. Based on the definition of *CPRU* problem and the monotonicity of $\overline{U}_k(\mathcal{H}_s)$, we can set the initial lower bound and upper bound of k in binary search as $k_{min} = 0$ and $k_{max} = min_{s_i\in S}P_i^{max}$, respectively. The while-loop (Lines 2-14) is a process of finding the maximum of k through binary search such that the size of $\mathcal{H}_s$ is not more than m. Let $\mathcal{H}'_s$ be the strategy set selected in each round of search. The while-loop (Lines 5-8) selects the charger from $\mathcal{H}_f \backslash \mathcal{H}'_s$ to $\mathcal{H}'_s$ until $\overline{U}_k(\mathcal{H}'_s) \geq k$ or the number of placed chargers is not smaller than the limitation m. In each iteration, we select the charger with the maximum marginal contribution to function $\overline{U}_k(\mathcal{H}'_s)$ over the unselected charger set $\mathcal{H}_f \backslash \mathcal{H}'_s$ (Line 6). The binary search terminates when $(k_{max} - k_{min}) < \gamma$, where $\gamma \in (0, 1)$ is the search accuracy.

Algorithm 3 Algorithm for *CPRU* Problem

Input: strategy space $\mathcal{H}_f$, set of sensor node S, search accuracy γ, maximum number of wireless chargers m
Output: strategy set of placed chargers $\mathcal{H}_s$

1: $k_{min} \leftarrow 0$; $k_{max} \leftarrow min_{s_i\in S}P_i^{max}$; $\mathcal{H}_s \leftarrow \emptyset$;
2: **while** $(k_{max} - k_{min}) \geq \gamma$ **do**
3: $k \leftarrow \frac{k_{min}+k_{max}}{2}$;
4: $\mathcal{H}'_s \leftarrow \emptyset$;
5: **while** $\overline{U}_k(\mathcal{H}'_s) < k$ **and** $\mathcal{H}'_s \neq \mathcal{H}_f$ **do**
6: $(o_j, \theta_j) \leftarrow \arg max_{(o_h,\theta_h)\in\mathcal{H}_f\backslash\mathcal{H}'_s}(\overline{U}_k(\mathcal{H}'_s \cup \{(o_h,\theta_h)\}) - \overline{U}_k(\mathcal{H}'_s))$;
7: $\mathcal{H}'_s \leftarrow \mathcal{H}'_s \cup \{(o_j, \theta_j)\}$;
8: **end while**
9: **if** $|\mathcal{H}'_s| > m$ **then**
10: $k_{max} \leftarrow k$
11: **else**
12: $k_{min} \leftarrow k$; $\mathcal{H}_s \leftarrow \mathcal{H}'_s$
13: **end if**
14: **end while**

Theorem 9. *The time complexity of algorithm for CPRU problem is* $O(\frac{n^5 m}{\gamma\epsilon^{-2}} \log min_{s_i\in S}P_i^{max})$.

Proof: Considering the search accuracy γ and search space $p_{max} - p_{min} = min_{s_i\in S}P_i^{max}$, the binary search (Lines 2-14) has $\frac{\log min_{s_i\in S}P_i^{max}}{\gamma}$ iterations. In each iteration, finding the placement strategy with the maximum marginal contribution (Line 6) takes $O(n|\mathcal{H}_f|)$ time. Since the maximum number of chargers can be placed is m, the while-loop (Lines 5-8) takes $O(nm|\mathcal{H}_f|)$ time. Thus, the running time of algorithm for *CPRU* is $O(\frac{nm|\mathcal{H}_f|}{\gamma} \log min_{s_i\in S}P_i^{max})$. Based on Lemma 2 and Lemma 3, the size of $\mathcal{H}_f$ is $O(K^2n^4)$. Based on Lemma 3, we have $K = O(\epsilon^{-1})$. Therefore, the time complexity of algorithm for *CPRU* problem is $O(\frac{n^5 m}{\gamma\epsilon^{-2}} \log min_{s_i\in S}P_i^{max})$. ■

6 Performance Evaluation

In this section, we conduct extensive simulations to evaluate the performance of *CPRC* algorithm and *CPRU* algorithm.

6.1 Performance Evaluation of CPRC Algorithm

For *CPRC* problem, we conduct area partition to partition the 2D plane to subareas. Afterwards, the dominating strategy extraction (Algorithm 1) is performed for each subarea. Finally, we execute the approximation algorithm for *CPRC* problem (Algorithm 2) based on the dominating strategies to obtain the strategy set of placed chargers.

Since there are no off-the-shelf robust charger placement algorithms for *CPRC* problem so far, we compare our solution with the following three randomized algorithms:

- *Randomized Position and Dominating Orientation (RPDO)*. *RPDO* places the charger iteratively, and randomly selects a position and a dominating orientation so long as the selected strategy can increase the coverage for at least one sensor node.
- *Randomized Position and Maximum Dominating Orientation (RPMDO)*. *RPMDO* improves *RPDO* by selecting the dominating orientation covering the most sensor nodes.
- *Randomized Position and Maximum Marginal Dominating Orientation (RPMMDO)* [42]. *RPMMDO* selects the dominating orientation with maximum marginal coverage, which is a widely used greedy criterion in covering problem with the goal of minimizing the number of subsets.

For our simulations, we uniformly distribute sensor nodes in a $60m \times 60m$ square area. The settings of parameters refer to the existing work [14], which optimizes the overall charging utility subject to the number of chargers. We will vary the value of the key parameters to explore the impacts on designed algorithms. Specifically, we set $\alpha = 100$, $\beta = 40$, $D = 6m$, $n = 100$, $A_s = \pi/2$ and $A_o = 2\pi/3$. The coverage demand λ_i of each sensor node s_i is a particular parameter of *CPRC* problem, which represents the robustness for resisting the wireless charger failure. In this paper, λ_i is a randomly selected integer from the interval [1, 3], where $\lambda_i = 1$ means there is no robustness, and $\lambda_i = 3$ represents the highest robustness. In the real world, it is robust enough when the sensor node is

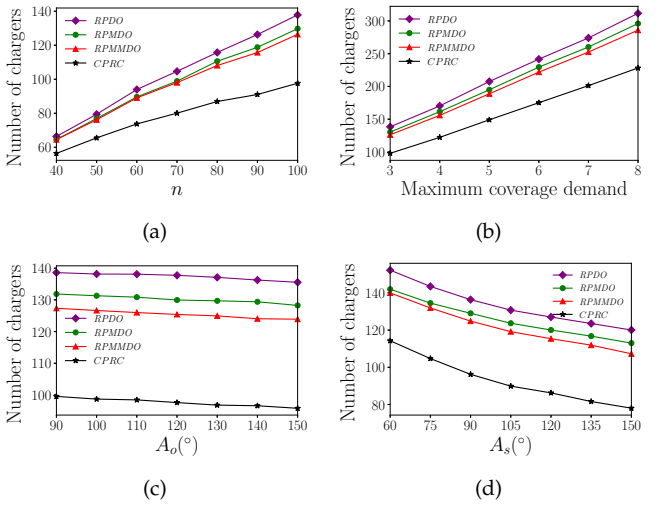

Fig. 8. Number of chargers. (a) Number of chargers vs. n. (b) Number of chargers vs. maximum coverage demand. (c) Number of chargers vs. A_o. (d) Number of chargers vs. A_s.

covered by 3 chargers. In our simulations, we vary the value of maximum coverage demand from 3 to 8. All the simulations are run on a Windows machine with Intel(R) Xeon(R) CPU E5-2603 v2 and 16 GB memory. Each measurement is averaged over 100 random topologies.

(1) Number of chargers. The *CPRC* problem optimizes the number of chargers with the constraint of robustness (coverage demand). As shown in Fig. 8(a), the number of chargers of all algorithms increases with n. *CPRC* outperforms *RPDO*, *RPMDO* and *RPMMDO* by 22.32%, 18.65%, and 17.48%, respectively, in terms of n averagely. The number of chargers of *CPRC* increases more slowly than the other algorithms, indicating that *CPRC* shows better expansibility. Then, we vary the coverage demand by varying the upper bound of the uniformly distribution, called maximum coverage demand, from 2 to 8. The results in Fig. 8(b) show that the number of chargers of all algorithms increases linearly with the maximum coverage demand. *CPRC* outperforms *RPDO*, *RPMDO* and *RPMMDO* by 28.09%, 23.95% and 21.47%, respectively, in terms of the maximum coverage demand averagely. Our simulation results in Fig. 8(c) shows that the number of chargers of all algorithms decreases slowly with the receiving angle A_o. This is because the sensor nodes with larger A_o can receive the power from more chargers, reducing the number of chargers. *CPRC* outperforms *RPDO*, *RPMDO* and *RPMMDO* by 28.91%, 24.99% and 22.18%, respectively, in terms of A_o averagely. Fig. 8(d) shows that the number of chargers of all algorithms decreases with the charging angle A_s. *CPRC* outperforms *RPDO*, *RPMDO* and *RPMMDO* by 29.35%, 24.91% and 22.65%, respectively, in terms of A_s averagely. The number of chargers of *CPRC* decreases faster than the other algorithms, thus, *CPRC* shows greater superiority with larger charging angles. The experiment results in Fig. 8 have shown that our algorithm can obtain the least chargers under various network settings, including different coverage demands. This indicates that our algorithm can meet the robustness with fewer chargers (lower cost).

(2) Running time. We can see from Fig. 9 that the

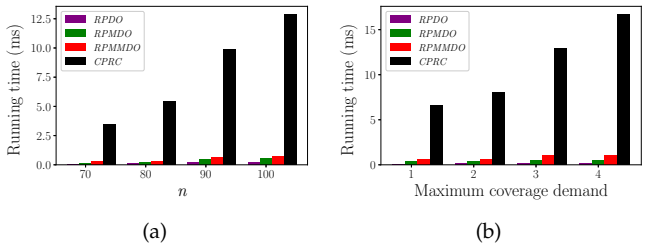

Fig. 9. Running time of *CPRC*. (a) Running time vs. n. (b) Running time vs. maximum coverage times.

running time of *CPRC* increases sharply with the number of sensor nodes, and increases almost linearly with the maximum coverage demand. The result is consistent with the time complexity analysis given in Theorem 3. *CPRC* can be terminated within 12.95 ms when $\lambda_i \in [1, 3]$ with 100 sensor nodes.

6.2 Performance Evaluation of CPRU Algorithm

For *CPRU* problem, we first use the piecewise constant function to obtain the approximation of charging power. Then, we conduct the area discretization. Afterwards, the dominating strategy extraction (Algorithm 1) is performed for each subarea. Finally, we execute the algorithm for *CPRU* problem (Algorithm 3) based on the dominating strategies to obtain the strategy set of placed chargers.

We compare our solution with the following two algorithms:

- *PLOT* [14]. *PLOT* selects the placement strategy with the maximum marginal total charging utility iteratively until m chargers are placed.
- *Maximizing Marginal Utility of the Worst (MMUW)*. *MMUW* selects the placement strategy with the maximum marginal charging utility of the senor node with the worst utility iteratively until m chargers are placed.

For our simulations, we set $\epsilon = 0.2$ and $\gamma = 0.001$, $n = 90$, $m = 100$ and $P_i^{max} = 0.14W$ for each $s_i \in S$. The other parameter settings are the same as those provided in Section 6.1. The search accuracy γ and approximation error ϵ are the particular parameters of the algorithm for *CPRU* problem. We set $\gamma = 0.001$, which is small enough to guarantee the accuracy of binary search. Moreover, we set $\epsilon = 0.2$ to guarantee the gap between approximation power and real power is small. Note that search accuracy and approximation error are two parameters to tradeoff the performance and running time. Setting small values of search accuracy and approximation error can obtain high performance but leads to long running time. We will vary the value of the key parameters to explore the impacts on designed algorithms.

(1) Charging utility. The *CPRU* problem optimizes the robustness (the minimum charging utility of all sensor nodes) subject to the number of chargers. As shown in Fig. 10(a), the charging utility of all three algorithms decreases with the increase of n since there will be more sensor nodes, which need to be charged. *CPRU* outperforms *PLOT* and *MMUW* by 120.11% and 54.61%, respectively, with different

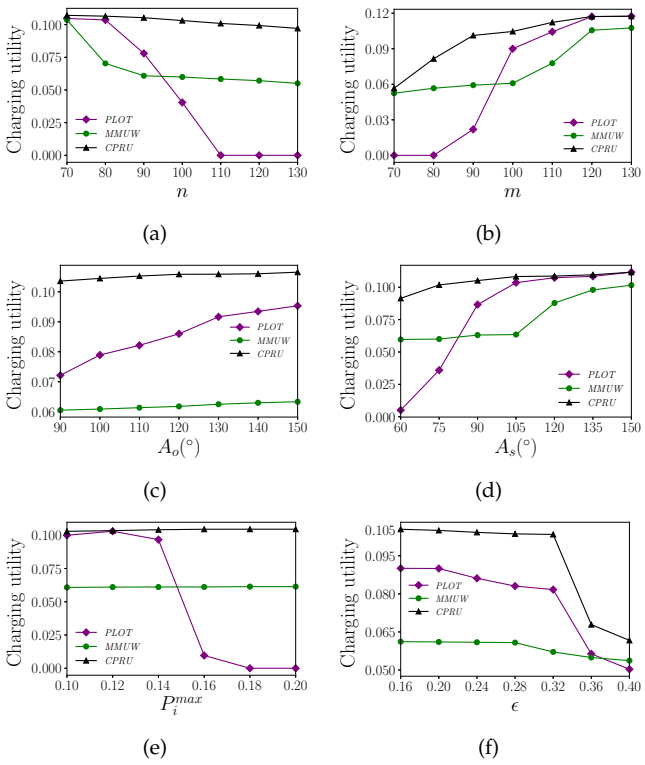

Fig. 10. Charging utility. (a) Charging utility vs. *n*. (b) Charging utility vs. *m*. (c) Charging utility vs. A_o. (d) Charging utility vs. A_s. (e) Charging utility vs. P_i^{max}. (f) Charging utility vs. ϵ.

values of n averagely. With a small n (less than 70), the charging utility of three algorithms is close to each other. This is because the default number of chargers is 100, and is sufficient to cover all sensor nodes. With a larger n, the difference of three algorithms becomes larger since the chargers are insufficient. When there are more than 110 sensor nodes, the charging utility of *PLOT* is zero because *PLOT* aims at maximizing the total utility rather than the minimum utility, therefore, some sensor nodes cannot be charged. We can see from Fig. 10(b) that the charging utility of all three algorithms decreases with the increase of m, and becomes stable when there are enough chargers (more than 100). This is because there is a maximum charging power for each sensor node, and increasing the number of chargers cannot help to increase the charging utility. *CPRU* outperforms *PLOT* and *MMUW* by 53.25% and 32.81%, respectively, with different values of m averagely. As shown in Fig. 10(c), when the receiving angle increases, the charging utility increases since the sensor nodes can receive power from more changers. *CPRU* outperforms *PLOT* and *MMUW* by 23.01% and 70.23%, respectively, with different values of A_o averagely. Similarly, as shown in Fig. 10(d), the charging utility increases with A_s, and *CPRU* outperforms *PLOT* and *MMUW* by 44.73% and 37.01%, respectively, with different values of A_o averagely. With the increase of the maximum charging power of sensor nodes, the charging utility of *CPRU* and *MMUW* increases slowly. We can see from Fig. 10(e), *CPRU* outperforms *PLOT* and *MMUW* by 80.87% and 64.77%, respectively, with different values of the maximum charging power averagely. However, the charging utility of *PLOT* decreases sharply when the maximum charging power is larger than 0.14. This is because *PLOT* aims to maximize the total charging utility rather than allocate the power evenly over all sensor nodes. When the sensor nodes receive higher power, some sensor nodes may not obtain any power. As shown in Fig. 10(f), the charging utility of all three algorithms decreases with the increase of ϵ. When ϵ is smaller than 0.32, the charging utility of *CPRU* can remain stable. *CPRU* outperforms *PLOT* and *MMUW* by 21.15% and 58.96%, respectively, with different values of ϵ averagely. The experiment results in Fig. 10 have shown that our algorithm can obtain the highest robustness under various network settings.

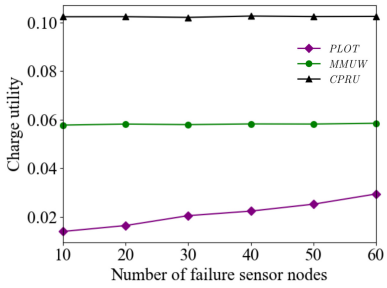

Fig. 11. Charging utility vs. number of failure sensor nodes.

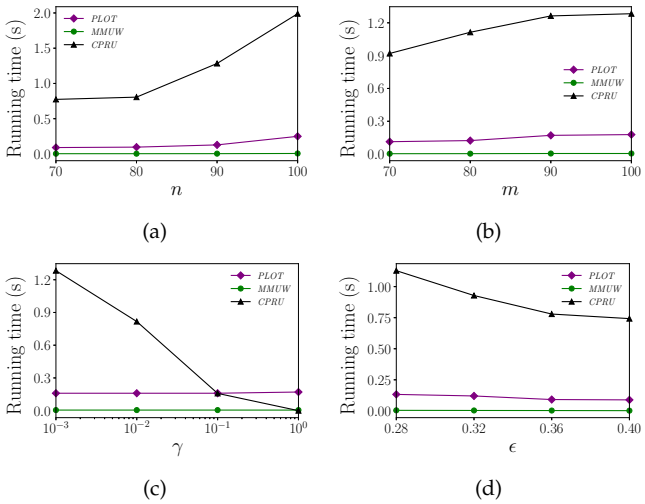

Fig. 12. Running time of *CPRU*. (a) Running time vs. n. (b) Running time vs. m. (c) Running time vs. γ. (d) Running time vs. ϵ.

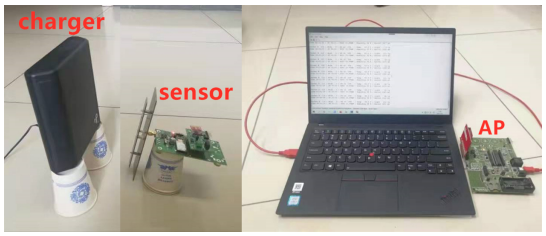

Fig. 13. Testbed.

(2) Charging utility with failure sensor nodes. To verify the robustness for resisting the sensor node failure, we have added the experiments to measure the minimum charging

utility of all sensor nodes with the varying number of failure sensor nodes from 20 to 60. To ensure that the normal sensor nodes are more than the failure sensor nodes, the total number of sensor nodes is set as 130. After obtaining the placement of chargers, we randomly remove some sensor nodes to simulate sensor node failure. We can see from Fig. 11 that the charging utility of *CPRU* and *MMUW* is stable with the increase of number of failure sensor nodes. This is because both *CPRU* and *MMUW* try to improve the minimum charging utility of sensor nodes, and the charging utility is evenly distributed among the sensor nodes in the rough. Thus, the sensor node failure has little impact on the charging utility. However, *PLOT* selects the placement strategy with the maximum marginal total charging utility iteratively, which may lead to great difference of charging utility. As a result, the charging utility increases with the increase of number of failure sensor nodes. Overall, *CPRU* outperforms *PLOT* and *MMUW* by 378.61% and 75.99% in terms of charging utility, respectively.

(3) Running time. We can see from Fig. 12(a) and Fig. 12(b) that the running time of all three algorithms increases with the increase of n or m. As shown in Fig. 12(c), the running time of *CPRU* decreases with the increasing search accuracy, nevertheless, *PLOT* and *MMUW* do not apply the binary search, and the running time remains unchanged. We can see from Fig. 12(d) that *CPRU* can be terminated within 1.28 s when $\epsilon = 0.32$ with 100 sensor nodes.

7 Field Experiemnts

We have conducted the field experiments to evaluate the proposed algorithms on the Lifetime Power Energy Harvesting Development Kit for Wireless Sensors (P2110-EVAL-01), which is a complete demonstration and development platform for creating battery-free wireless sensors (passive wireless sensor tags) powered by RF energy (radio waves) [12]. The wireless sensor nodes are powered by the P2110 Powerharvester Receiver, which converts RF energy into DC power. In this kit, the TX91501 transmitter is the source of RF energy (915MHz). The communication from the sensor nodes to the Access Point (AP) is 2.4GHz using 802.15.4-compliant radios. When the sensor nodes receive energy from chargers, they begin to work and send data packets, including temperature, humidity, light and received power information, to the AP. The AP is connected to the laptop through the USB interface, then we can read power and data through HyperTerminal called CoolTerm [43].

7.1 Field Experiments of CPRC Algorithm

We conduct the experiments in a $4m \times 4m$ square area, where four sensor nodes are placed at the randomly selected positions in the area with coordinates (1.72, 0.95), (2.75, 2.16), (0.84, 1.94), and (3.22,1.91), and the coverage demands 2, 1, 2, and 1.

The detailed strategies of four algorithms are shown in TABLE 2 and Fig. 14. We can see that *CPRC* only uses 5 chargers to cover all sensor nodes. However, the number of chargers of *RPDO*, *RPMDO* and *RPMMDO* is 11, 8, and 9, respectively.

TABLE 2
Charger Placement Strageties of Four Algorithms

#	*RPDO*	*RPMDO*	*RPMMDO*	*CPRC*
1	$\langle(3.27, 1.93), 11°\rangle$	$\langle(1.41, 1.08), 101°\rangle$	$\langle(1.41, 1.08), 101°\rangle$	$\langle(3.09, 2.44), 11°\rangle$
2	$\langle(3.43, 1.72), 2°\rangle$	$\langle(0.82, 1.95), 95°\rangle$	$\langle(0.82, 1.95), 95°\rangle$	$\langle(1.41, 1.08), 101°\rangle$
3	$\langle(3.52, 1.66), 3°\rangle$	$\langle(3.52, 1.66), 3°\rangle$	$\langle(3.42, 1.72), 2°\rangle$	$\langle(1.37, 1.15), 97°\rangle$
4	$\langle(3.09, 2.44), 42°\rangle$	$\langle(1.37, 1.15), 97°\rangle$	$\langle(3.05, 2.03), 11°\rangle$	$\langle(0.82, 1.95), 95°\rangle$
5	$\langle(3.05, 2.03), 11°\rangle$	$\langle(3.27, 1.93), 11°\rangle$	$\langle(3.05, 2.03), 94°\rangle$	$\langle(0.64, 1.59), 142°\rangle$
6	$\langle(1.41, 1.08), 101°\rangle$	$\langle(3.42, 1.72), 2°\rangle$	$\langle(3.27, 1.93), 11°\rangle$	
7	$\langle(3.27, 1.93), 34°\rangle$	$\langle(3.05, 2.03), 11°\rangle$	$\langle(3.09, 2.44), 42°\rangle$	
8	$\langle(0.82, 1.95), 95°\rangle$	$\langle(0.64, 1.59), 142°\rangle$	$\langle(1.37, 1.15), 97°\rangle$	
9	$\langle(0.64, 1.59), 142°\rangle$		$\langle(0.64, 1.59), 142°\rangle$	
10	$\langle(3.05, 2.03), 94°\rangle$			
11	$\langle(1.37, 1.15), 97°\rangle$			

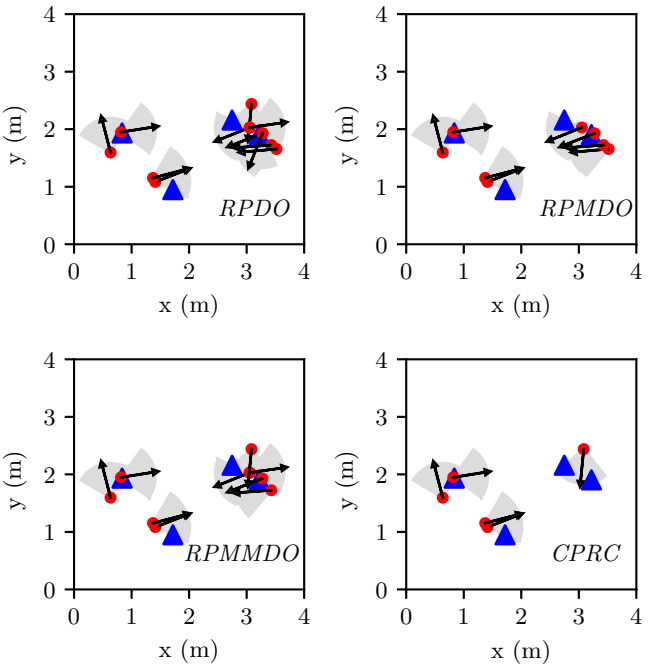

Fig. 14. Charger placement strategies of *RPDO*, *RPMDO*, *RPMMDO* and *CPRC*. The blue triangles represent the sensor nodes, and the red dots represent the chargers.

7.2 Field Experiments of CPRU Algorithm

We conduct the experiments in a $4m \times 4m$ square area, where six sensor nodes are placed at the randomly selected positions in the area with coordinates (1.32,1.65), (1.07, 1.26), (2.89, 2.38), (1.53, 1.19), (0.97, 1.95), and (1.06, 2.91). Note that we set $\epsilon = 0.2$, $\gamma = 0.001$, $m = 8$ and $P_i^{max} = 0.14W$ for each sensor node.

TABLE 3
Charger Placement Strageties of Three Algorithms

#	*PLOT*	*MMUW*	*CPRU*
1	$\langle(1.01, 1.26), 108°\rangle$	$\langle(1.32, 1.65), 2°\rangle$	$\langle(1.01, 1.26), 108°\rangle$
2	$\langle(1.32, 1.65), 2°\rangle$	$\langle(1.06, 1.27), 72°\rangle$	$\langle(1.01, 1.60), 117°\rangle$
3	$\langle(1.06, 1.27), 72°\rangle$	$\langle(2.85, 2.54), 74°\rangle$	$\langle(2.85, 2.54), 74°\rangle$
4	$\langle(1.01, 1.60), 117°\rangle$	$\langle(1.12, 2.54), 162°\rangle$	$\langle(1.12, 2.54), 162°\rangle$
5	$\langle(1.32, 1.65), 51°\rangle$	$\langle(1.47, 1.14), 133°\rangle$	$\langle(1.32, 1.65), 51°\rangle$
6	$\langle(2.85, 2.54), 74°\rangle$	$\langle(0.93, 1.74), 153°\rangle$	$\langle(1.42, 2.77), 12°\rangle$
7	$\langle(1.12, 2.54), 162°\rangle$	$\langle(1.42, 2.78), 12°\rangle$	$\langle(1.32, 1.65), 2°\rangle$
8	$\langle(1.42, 2.77), 12°\rangle$	$\langle(2.32, 2.26), 118°\rangle$	$\langle(2.32, 2.26), 118°\rangle$

The detailed strategies of three algorithms are shown in

TABLE III and Fig. 15. Fig. 16 shows the charging utility for each sensor node for the three algorithms. We can see that our algorithm *CPRU* outperforms *PLOT* and *MMUW* by at least 68.97% and 58.06%, respectively. Specifically, the sensor node 3 has the minimum charging utility 0.058 in *PLOT*. The sensor node 2 has the minimum charging utility 0.062 in MMUW, and the sensor node 4 has the minimum charging utility 0.098 in *CPRU*.

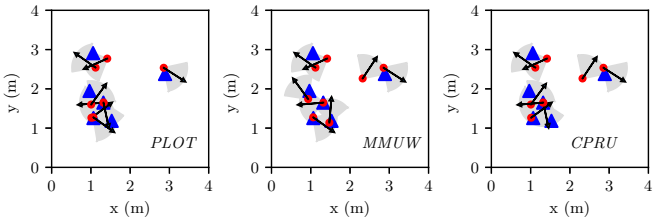

Fig. 15. Charger placement strategies of *PLOT*, *MMUW* and *CPRU*. The blue triangles represent the sensor nodes, and the red dots represent the chargers.

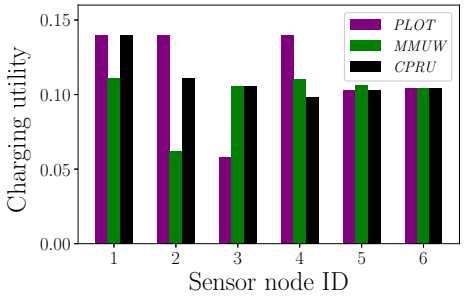

Fig. 16. Charging utility of sensor nodes.

8 Discussion

Both *CPRC* and *CPRU* need to place the wireless chargers in the specified positions. Therefore, in the actual implementation, we need to consider how to move the wireless chargers to these target positions. Since the moving of wireless chargers needs additional cost, it is necessary to minimize the total moving distance. If all the wireless chargers are concentrated in an initial position, we only need to move the wireless chargers directly to the target positions. However, in actual sensor networks, the wireless chargers are often distributed in different positions. For example, when the state of sensor network or the placement algorithm changes, we should schedule the moving of wireless chargers to the target positions with objective of minimizing the total moving distance. This problem is actually the unbalanced assignment problem, which can be solved by *Hungarian* algorithm [44].

9 Conclusion

In this paper, we have studied the fundamental issue of robust fault-tolerant placement of wireless chargers for directional charging. The *CPRC* problem with continuous and infinite constraints has been formulated for resisting the wireless charger failure. We have transformed the problem to the equivalence integer program problem without performance loss by area partition and dominating strategy extraction. We show that the greedy algorithm for set cover problem can hold the logarithmic approximation ratio for our *CPRC* problem. Moreover, we have formulated the *CPRU* problem for resisting the sensor node failure. Through the techniques of charging power approximation, area discretization and dominating strategy extraction, the continuous search space of strategies of chargers has been reduced to a limited number of strategies without performance loss. We have transformed the reformulated *CPRU* problem, and solved the problem of maximizing the minimum of multiple submodular functions with cardinality lower bound through the integrating of approximation algorithm for submodular covering problem and binary search. The results of both simulations and field experiments show that the proposed algorithms for *CPRC* and *CPRU* can outperform the comparison algorithms by at most 29.35% and 120.11%, respectively.

Acknowledgment

This work has been supported in part by the National Natural Science Foundation of China (No. 61872193, 62072254, 62272237, 62171217).

References

[1] *Wireless Power Consortium.* Accessed: 2021.[Online]. Available: https://www.wirelesspowerconsortium.com/about/about-wpc.
[2] X. Lu, P. Wang, D. Niyato, D. I. Kim and Z. Han, "Wireless Charging Technologies: Fundamentals, Standards, and Network Applications," *IEEE Communications Surveys & Tutorials*, vol. 18, no. 2, pp. 1413- 1452, 2016.
[3] *Wireless Identification and Sensing Platform.* Accessed: 2021. [Online]. Available: http://www.terabits.cn/product.
[4] J. Xu, S. Hu, S. Wu, K. Zhou, H. Dai and L. Xu, "Cooperative Charging as Service: Scheduling for Mobile Wireless Rechargeable Sensor Networks," in *Proc. IEEE ICDCS*, 2021, pp. 685-695.
[5] Y. Jin, J. Xu, S. Wu, L. Xu and D. Yang, "Enabling the Wireless Charging via Bus Network: Route Scheduling for Electric Vehicles," *IEEE Transactions on Intelligent Transportation Systems*, vol. 22, no. 3, pp. 1827-1839, 2021.
[6] Y. Jin, J. Xu, S. Wu, L. Xu, D. Yang and K. Xia. "Bus network assisted drone scheduling for sustainable charging of wireless rechargeable sensor network," *Journal of Systems Architecture*, vol. 116, doi:10.1016/j.sysarc.2021.102059, 2021.
[7] Z. Cheng, Y. Lei, K. Song and C. Zhu. "Design and loss analysis of loosely coupled transformer for an underwater high-power inductive power transfer system," *IEEE Transactions on Magnetics*, vol. 51, no. 7, pp. 1-10, 2015.
[8] *Wireless Power Transfer Market.* Accessed: 2021. [Online]. Available: https://www.electronics.ca
[9] A. Famili and A. Stavrou, "Eternal Flying: Optimal Placement of Wireless Chargers for Nonstop Drone Flights," in *Proc. IEEE ICECET*, 2022, pp. 1-6.
[10] Y. Li, Y. Chen, C. S. Chen, Z. Wang and Y. H. Zhu, "Charging while Moving: Deploying Wireless Chargers for Powering Wearable Devices," *IEEE Transactions on Vehicular Technology*, vol. 67, no. 12, pp. 11575-11586, 2018.
[11] A. U. Sarma, K. P. V. Jeya, V. A. Vigneshwar and K. S. Anusha, "Optimal Placement Of Wireless Chargers In Indoor Environment Using Clustering Algorithm," in *Proc. IEEE ICOEI*, 2019, pp. 1087-1094.
[12] *Powercast.* Accessed: 2021. [Online]. Available: https://www.powercastco.com.
[13] *Directional antenna.* Accessed: 2021. [Online]. Available: https://en.jinzhao.wiki/wiki/Directional_antenna.
[14] H. Dai, X. Wang, A. Liu, H Ma and G. Chen, "Wireless charger placement for directional charging," *IEEE/ACM Transactions on Networking*, vol. 26, no. 4, pp. 1865-1878, 2018.

[15] H. Dai, Y. Xu, G. Chen, W. Dou, C. Tian, X. Wu and T. He, "ROSE: Robustly Safe Charging for Wireless Power Transfer," *IEEE Transactions on Mobile Computing*, vol. 21, no. 6, pp. 2180-2197, 2022.

[16] X. Wang , H. Dai, H. Huang , Y. Liu and W. Dou, "Robust Scheduling for Wireless Charger Networks," in *Proc. IEEE INFOCOM*, 2019, pp. 1877-1886.

[17] *TX91501 Wireless Chargers*. Accessed: 2018. [Online]. Available: http://www.powercastco.com/pdf/tx91501-manual.pdf

[18] *Failure of electronic components.* Accessed: 2021. [Online]. Available: https://en.jinzhao.wiki/wiki/Failure_of_electronic_components

[19] B. Song, M. H. Azarian and M. G. Pecht, "Impact of Dust on Printed Circuit Assembly Reliability," in *Proc. IPC APEX EXPO*. 2012, pp. 1643-1659.

[20] H. Wei, G. Wang, Q. Shi and X. Tian, "Research on Electronic Equipment Damage Simulation in Explosion Impact Vibration Environment," *Acta Armamentarii*, vol. 33, no. 1, pp. 13-18, 2012.

[21] S. Wu, H. Dai, L. Liu, L. Xu, F. Xiao and J. Xu, "Cooperative Scheduling for Directional Wireless Charging with Spatial Occupation," *IEEE Transactions on Mobile Computing*, 10.1109/TMC.2022.3214979, 2022.

[22] S. Wu, H. Dai, L. Xu, L. Liu, F. Xiao and J. Xu, "Comprehensive Cost Optimization for Charger Deployment in Multihop Wireless Charging," *IEEE Transactions on Mobile Computing*, vol. 22, no. 8, pp. 4563-4577, 2023.

[23] A. V. Sutar, V. Dighe, P. Karavkar, P. Mhatre, and V. Tandel, "Solar Energy based Mobile Charger Using Inductive Coupling Transmission," in *Proc. IEEE ICICCS*, 2020, pp. 995-1000.

[24] E. Boshkovska, D. W. K. Ng, N. Zlatanov and R. Schober, "Practical Non-Linear Energy Harvesting Model and Resource Allocation for SWIPT Systems," *IEEE Communications Letters*, vol. 19, no. 12, pp. 2082-2085, 2015.

[25] D. Kumar, P. K. Singya, K. Choi and V. Bhatia, "SWIPT Enabled Cooperative Cognitive Radio Sensor Network with Non-Linear Power Amplifier," *IEEE Transactions on Cognitive Communications and Networking*, doi: 10.1109/TCCN.2023.3269511, 2023.

[26] J. Baek, S. I. Han and Y. Han, "Optimal UAV Route in Wireless Charging Sensor Networks," *IEEE Internet of Things Journal*, vol. 7, no. 2, pp. 1327-1335, 2020.

[27] S. Wu, L. Xu, H. Dai, L. Liu, F. Xiao and J. Xu, "Optimizing Comprehensive Cost of Charger Deployment in Multi-hop Wireless Charging," *ACM Transactions on Sensor Networks*, vol. 19, no. 4, pp. 1-24, 2023.

[28] X. Ding, J. Guo, Y. Wang, D. Li and W. Wu, "Task-driven charger placement and power allocation for wireless sensor networks," *Ad Hoc Networks*, vol. 19, no. 1, pp. 48-64, 2021.

[29] X. Ding, J. Guo, D. Li and W. Wu, "Optimal wireless charger placement with individual energy requirement," *Theoretical Computer Science*, vol. 857, pp.16-28, 2021.

[30] X. Ding, G. Sun, Y. Wang, C. Luo, D. Li, W. Chen and Q. Hu, "Cost-Minimum Charger Placement for Wireless Power Transfer," in *Proc. IEEE ICCCN*, 2019, pp. 1-9.

[31] W. Xu, W. Liang, H. Kan, Y. Xu and X. Zhang, "Minimizing the Longest Charge Delay of Multiple Mobile Chargers for Wireless Rechargeable Sensor Networks by Charging Multiple Sensors Simultaneously," in *Proc. IEEE ICDCS*, 2019, pp. 881-890.

[32] Y. Ma, W. Liang and W. Xu, "Charging utility maximization in wireless rechargeable sensor networks by charging multiple sensors simultaneously," *IEEE/ACM Transactions on Networking*, vol. 26, no. 4, pp. 1591-1604, 2018.

[33] W. Xu, W. Liang, X. Jia, Z. Xu, Z. Li and Y. Liu, "Maximizing Sensor Lifetime with the Minimal Service Cost of a Mobile Charger in Wireless Sensor Networks," *IEEE Transaction on Mobile Computing*, vol. 17, no. 11, pp. 1863-1876, 2018.

[34] S. Priyadarshani, A. Tomar, and P. K. Jana, "An efficient partial charging scheme using multiple mobile chargers in wireless rechargeable sensor networks," *Ad Hoc Networks*, vol. 113, no. 1. pp. 102407, 2021.

[35] C. Lin, F. Gao, H. Dai, J. Ren, L. Wang and Guo Wu, "Maximizing Charging Utility with Obstacles through Fresnel Diffraction Model", *in Proc. IEEE INFOCOM*, 2020, pp. 2046-2055.

[36] *Overload protection*. Accessed: 2021. [Online]. Available: https://en.jinzhao.wiki/wiki/Power_supply#Overload_protection

[37] S. Rajagopalan and V. Vazirani. "Primal-dual RNC approximation algorithms for (multi)-set (multi)-cover and covering integer programs," in *Proc. IEEE FOCS*, 1993, pp.322-331.

[38] U. Feige, "A threshold of ln n for approximating set cover," *Journal of the ACM*, vol. 45, no. 4, pp. 634-652, 1998.

[39] R. G. Michael and S. J. David, "Computers and intractability: a guide to the theory of np-completeness," *Siam Review*, vol. 24, no. 1, pp. 90, 1982.

[40] *Submodular set function.* Accessed: 2021. [Online]. Available: https://en.wikipedia.org/wiki/Submodular_set_function.

[41] G. L. Nemhauser, L. A. Wolsey and M. L. Fisher, "An analysis of approximations for maximizing submodular set functions,"*Mathematical Programming*, vol. 14, no. 1, pp. 265-294, 1978.

[42] N. Wang, J. Wu and H. Dai, "Bundle Charging: Wireless Charging Energy Minimization in Dense Wireless Sensor Networks," in *Proc. IEEE ICDCS*, 2019, pp. 810-820.

[43] *Roger Meier.* Accessed: 2021. [Online]. Available: http://freeware.the-meiers.org/.

[44] H. Kuhn, "The Hungarian Method for the assignment problem", *Naval Research Logistics Quarterly*, vol. 2, no. 1-2, pp. 83-97, 1955.

Jia Xu (M'15, SM'21) received the M.S. degree in School of Information and Engineering from Yangzhou University, Jiangsu, China, in 2006 and the PhD. Degree in School of Computer Science and Engineering from Nanjing University of Science and Technology, Jiangsu, China, in 2010. He is currently a professor in the School of Computer Science at Nanjing University of Posts and Telecommunications. He was a visiting Scholar in the Department of Electrical Engineering & Computer Science at Colorado School of Mines from Nov. 2014 to May. 2015. His main research interests include crowdsourcing, edge computing and wireless sensor networks. Prof. Xu has served as the PC Co-Chair of SciSec 2019, Publicity Co-Chair of SciSec 2021 and SciSec 2022, Organizing Chair of ISKE 2017, TPC member of IEEE Globecom, IEEE ICC, IEEE MASS, IEEE ICNC, and IEEE EDGE.

Kaijun Zhou received the bachelor's degree in School of Computer Science from Nanjing University of Posts and Telecommunications, Jiangsu, China, in 2019. He is currently a graduate student in the School of Computer Science at Nanjing University of Posts and Telecommunications. His main research interest is wireless rechargeable sensor network.

Sixu Wu received the bachelor's degree in School of Computer Science from Nanjing University of Posts and Telecommunications, Jiangsu, China, in 2019. He is currently a doctoral student in the School of Computer Science at Nanjing University of Posts and Telecommunications. His main research interest is wireless rechargeable sensor network.

Haipeng Dai (M'14, SM'22) received the B.S. degree in the Department of Electronic Engineering from Shanghai Jiao Tong University, Shanghai, China, in 2010, and the Ph.D. degree in the Department of Computer Science and Technology in Nanjing University, Nanjing, China, in 2014. His research interests are mainly in the areas of data mining, Internet of Things, and mobile computing. He is an associate professor in the Department of Computer Science and Technology in Nanjing University. His research papers have been published in many prestigious conferences and journals such as ACM VLDB, IEEE ICDE, ACM SIGMETRICS, ACM MobiSys, ACM MobiHoc, ACM UbiComp, IEEE INFOCOM, IEEE ICDCS, IEEE ICNP, IEEE SECON, IEEE IPSN, IEEE JSAC, IEEE/ACM TON, IEEE TMC, IEEE TPDS, IEEE TDSC, and IEEE TOSN. He is an IEEE and ACM member. He serves/ed as Poster Chair of the IEEE ICNP'14, Track Chair of the ICCCN'19 and the ICPADS'21, TPC member of the ACM MobiHoc'20-21, IEEE INFOCOM'20-22, IEEE ICDCS'20-21, IEEE ICNP'14, IEEE IWQoS'19-21, IEEE IPDPS'20'22 and IEEE MASS'18-19. He received Best Paper Award from IEEE ICNP'15, Best Paper Award Runner-up from IEEE SECON'18, and Best Paper Award Candidate from IEEE INFOCOM'17.

Lijie Xu received his Ph.D. degree in the Department of Computer Science and Technology from Nanjing University, Nanjing, in 2014. He was a research assistant in the Department of Computing at the Hong Kong Polytechnic University, Hong Kong, from 2011 to 2012. He is currently an associate professor in the School of Computer Science at Nanjing University of Posts and Telecommunications, Nanjing. His research interests are mainly in the areas of wireless sensor networks, ad-hoc networks, mobile and distributed computing, and graph theory algorithms.

Linfeng Liu (M'13) received the B. S. and Ph. D. degrees in computer science from the Southeast University, Nanjing, China, in 2003 and 2008, respectively. At present, he is a Professor in the School of Computer Science and Technology, Nanjing University of Posts and Telecommunications, China. His main research interests include the areas of vehicular ad hoc networks, wireless sensor networks and multi-hop mobile wireless networks. He has published more than 80 peer-reviewed papers in some technical journals or conference proceedings, such as IEEE TMC, IEEE TPDS, ACM TAAS, IEEE TSC, IEEE TVT, IEEE IoTJ, Computer Networks, Elsevier JPDC.